

Single Crystal X-Ray Diffraction Studies of Synthetic (Co,Mg)-Olivine Solid Solutions

Dan Boström

Department of Inorganic Chemistry, University of Umeå, S-901 87 Umeå, Sweden

Boström, D., 1989. Single Crystal X-Ray Diffraction Studies of Synthetic (Co,Mg)-Olivine Solid Solutions. – *Acta Chem. Scand.* 43: 121–127.

The structures of seven (Co,Mg)-olivine single crystals together with the Co_2SiO_4 end member have been investigated by X-ray diffraction methods. The crystals were synthesized at 900 °C in a high-temperature solution of Li_2MoO_4 . The intracrystalline partitioning of Mg^{2+} and Co^{2+} has been determined by least-squares refinement of the occupancies of the two octahedral sites. The K_D values (K_D is the intracrystalline distribution constant), which vary between 4.5 and 5.7, show only small compositional dependence. Octahedral geometric properties can in general be correlated with the content of each octahedron.

The intracrystalline distribution of divalent cations within the olivine structure has been the subject of many studies in recent years. Data relating to ordering over the two non-equivalent M1 and M2 octahedral sites are thus available for several olivine solid solutions (see Refs. 1 and 2 for a general survey).

A number of 3d transition metal ions form complete solid solutions together with Mg_2SiO_4 (forsterite), e.g. Fe^{2+} , Co^{2+} and Ni^{2+} . In the $(\text{Fe},\text{Mg})_2\text{SiO}_4$ solid solution, the divalent cations are almost randomly distributed, small preferences for Fe^{2+} in the M1 site being reported.^{3–5} The $(\text{Ni},\text{Mg})_2\text{SiO}_4$ solid solution on the other hand exhibits considerable ordering effects^{6–8} and Ni^{2+} shows a strong preference for the M1 site. The $(\text{Co},\text{Mg})_2\text{SiO}_4$ solid solution series is also strongly ordered, with Co^{2+} concentrated at the M1 site, though to a lesser extent than in the (Ni,Mg) -olivine. Ghose and Wan⁹ investigated a $(\text{Co}_{0.55}, \text{Mg}_{0.45})_2\text{SiO}_4$ single crystal synthesized at 1150 °C and 10 kbar, and obtained a K_D value of 4.6 calculated from the refined occupancies ($K_D = [\text{Co}_{\text{M}1}][\text{Mg}_{\text{M}2}]/[\text{Co}_{\text{M}2}][\text{Mg}_{\text{M}1}]$, where the symbols within the square brackets represent the fractional occupancy of the M1 and M2 sites by Co^{2+} and Mg^{2+}). Recently Miyake *et al.*¹⁰ have performed a systematic study of five (Co,Mg)-olivine single crystals with different compositions. These were synthesized at 1540 °C using a floating-zone technique. The intracrystalline distribution coefficient, K_D was found to vary between 3.08 and 5.39. No information is available, however, as to the cooling history of the crystals. It is therefore not possible to assign the K_D values obtained to an effective equilibrium temperature.

Recent results⁸ have shown that the cation distribution in the (Ni,Mg) -olivine single crystals, synthesized at 900 °C, varies with cation composition. The ordering appeared to have a minimum value at the composition $X(\text{Ni}^{2+}) = 0.60$, and to increase towards the end members, especially

on the Mg_2SiO_4 side. The present investigation of the $(\text{Co},\text{Mg})_2\text{SiO}_4$ -olivine solid solution series was undertaken to discover whether this correlation of K_D with composition is significant only for the (Ni,Mg) -olivine or can also be found for other transition metal olivines.

To avoid zoning in the crystals and to ensure equilibrium cation distributions, the temperature was kept constant at 900 °C during the synthesis.

Experimental

Single crystal synthesis. The crystals used in this investigation were grown in a Li_2MoO_4 solution. The starting materials, as given in Table 1, were mixed and placed in an unsealed Pt crucible. The crystals so prepared were rapidly quenched by cooling the crucibles in ice. Further details of the synthesis are given in Table 1.

The composition of the crystals was analyzed by a microprobe technique, and the results are given in Table 1. For details of the analytical procedure, see Ref. 11. The compositions showed some deviation from those calculated on the basis of the starting materials. The crystals were all lower in Co^{2+} -content than expected.

X-Ray data collection. The dimensions of the orthorhombic unit cell were determined by least-squares refinement of 20 to 24 automatically centered $\text{MoK}\alpha_1$ reflections with $\sin \theta/\lambda \approx 1.1 \text{ \AA}^{-1}$, to ensure good separation of the α_1 and α_2 peaks. X-Ray data were collected at room temperature using a Nicolet R3 four-circle diffractometer, with graphite-monochromated $\text{MoK}\bar{\alpha}$ radiation ($\lambda = 0.71069 \text{ \AA}$) and θ -2 θ scan mode ($4.6^\circ \leq 2\theta \leq 80^\circ$). The scan speed was varied between 2.0 and 6.0 deg min⁻¹. Conventional background-peak-background measurement of intensity was applied. Lorentz, polarization and absorption corrections were also made, the latter by an empirical procedure sup-

Table 1. Crystal synthesis.

	Starting materials/g							
	1	2	3	4	5	6	7	8
Li_2CO_3	6.3765	6.3765	6.3765	6.3765	6.3765	6.3765	6.3765	6.3765
MoO_3	12.4216	12.4216	12.4216	12.4216	12.4216	12.4216	12.4216	12.4216
CoO	0.2050	0.3340	0.4488	0.6220	1.5736	1.8342	2.0329	2.2485
MgO	0.4381	0.3336	0.2414	0.0863	0.4558	0.2466	0.0608	
SiO_2	0.4092	0.3825	0.3598	0.3217	0.9706	0.9192	0.9063	0.9015
Duration d	8	7	8	7	9	7	7	6
Temperature °C	900(2)	900(1)	898(1)	902(1)	900(1)	902(2)	200(1)	901(1)
Composition $X(\text{Co}^{2+})$	0.175	0.258	0.377	0.503	0.604	0.745	0.929	1.000

Table 2. Crystal data.

	$X(\text{Co}^{2+})$							
	0.175	0.258	0.377	0.503	0.604	0.745	0.929	1.000
Cell dimensions								
$a \text{ \AA}$	4.7616(5)	4.7659(5)	4.7687(5)	4.7723(4)	4.7750(5)	4.7782(5)	4.7815(8)	4.7827(4)
$b \text{ \AA}$	10.2161(14)	10.2292(8)	10.2409(8)	10.2535(7)	10.2648(8)	10.2750(9)	10.2952(13)	10.3040(8)
$c \text{ \AA}$	5.9826(7)	5.9855(5)	5.9872(5)	5.9884(4)	5.9914(5)	5.9940(6)	5.9970(8)	6.0011(5)
$V \text{ \AA}^3$	291.03 (6)	291.80 (4)	292.39 (5)	293.03 (4)	293.67 (5)	294.28 (5)	295.21 (7)	295.74 (4)
Number of reflections								
with $ I > 3\sigma(I)$	869	822	878	817	870	874	888	859
Final value of R^a	2.17	2.21	2.18	2.14	4.03	3.31	3.56	3.27
R_w^b	3.32	2.85	2.87	2.56	5.21	4.46	4.68	4.38
K_D value	4.50 (6)	5.20 (6)	5.47 (4)	4.98 (3)	5.7 (3)	5.6 (1)	4.8 (4)	

$$^a R = [\sum(|F_o| - |F_c|)/\sum|F_o|] \cdot 100 \%. \quad ^b R_w = [\sum w(|F_o| - |F_c|)^2 / \sum w F_o^2]^{1/2} \cdot 100 \%.$$

plied with the Nicolet R3 crystallographic system. Additional experimental details are listed in Table 2.

Refinements. The refinements were carried out in the space group $Pbnm$ using the least-squares program UPALS.¹² Scattering factors for neutral atoms with corrections for anomalous dispersion were taken from Ref. 13. The compositions of the solid solution olivines were constrained to the microprobe analysis. In the final refinement cycles, one overall scale factor, one isotropic secondary extinction parameter, positional and anisotropic temperature factors together with occupancy factors for M1 and M2, were varied. The fractional coordinates obtained for the various compositions, together with occupancy factors and the isotopic equivalence of the anisotropic temperature factors, are listed in Table 3. Anisotropic temperature factors and interatomic angles are listed in Tables 4 and 5, respectively.

Results and discussion

The olivine structure is well known and has been discussed in detail by several authors; the interested reader is referred to Brown¹ for a detailed description of the structure.

In Figs. 3–6, the parameter values for the end member Mg_2SiO_4 are taken from Ref. 8.

Cation distribution. The K_D values given in Table 2 and plotted in Fig. 1a are calculated from the occupancy factors given in Table 3. The calculated standard deviations of the K_D values are ≤ 0.1 , except for the compositions with $X(\text{Co}^{2+})$ 0.604 and 0.929, where they are 0.3 and 0.4, respectively. The K_D values for the various olivines vary between 4.5 and 5.7, which are slightly higher than the values given by Miyake *et al.*¹⁰ The latter probably reflect the ordering situation at a temperature higher than 900 °C, and would therefore be expected to be lower. In contrast to the strong K_D compositional dependence for $(\text{Ni}, \text{Mg})_2\text{SiO}_4$ solid solution synthesized under equivalent conditions,⁸ the present K_D values exhibit only small compositional variation.

The three independent studies performed with $(\text{Co}, \text{Mg})_2\text{SiO}_4$ single crystals all give K_D values between 3.08 and 6.46. This consistent picture of the ordering situation in (Co, Mg) -olivine is somewhat surprising, considering the very different conditions for synthesis of the crystals investigated. One explanation could be that the temperature

Table 3. Atomic fractional coordinates, isotropic temperature factors^a (B in \AA^2) and occupancy factors^b (G)

	$X(\text{Co}^{2+})$							
Atom	0.175	0.258	0.377	0.503	0.604	0.745	0.929	1.000
M1	0.0	0.0	0.0	0.0	0.0	0.0	0.0	0.0
	<i>y</i>	0.0	0.0	0.0	0.0	0.0	0.0	0.0
	<i>z</i>	0.0	0.0	0.0	0.0	0.0	0.0	0.0
	<i>B</i>	0.42 (1)	0.39 (1)	0.43 (1)	0.44 (1)	0.54 (1)	0.50 (1)	0.51 (1)
Mg <i>G</i>	0.364 (1)	0.299 (1)	0.218 (1)	0.153 (1)	0.101 (4)	0.053 (1)	0.013 (1)	0.500 (0)
Co <i>G</i>	0.136 (1)	0.201 (1)	0.282 (1)	0.347 (1)	0.399 (4)	0.447 (1)	0.487 (1)	0.500 (0)
M2	<i>x</i>	0.9913(1)	0.9910(1)	0.9911(1)	0.9910(1)	0.9910(1)	0.9911(1)	0.9912(1)
	<i>y</i>	0.2771(1)	0.2769(1)	0.2768(1)	0.2766(1)	0.2766(1)	0.2765(1)	0.2765(1)
	<i>z</i>	0.25	0.25	0.25	0.25	0.25	0.25	0.25
	<i>B</i>	0.43 (1)	0.38 (1)	0.44 (1)	0.44 (1)	0.48 (1)	0.50 (1)	0.50 (1)
Mg <i>G</i>	0.461 (1)	0.443 (1)	0.405 (1)	0.344 (1)	0.295 (4)	0.202 (1)	0.058 (1)	0.5
Co <i>G</i>	0.039 (1)	0.057 (1)	0.095 (1)	0.156 (1)	0.205 (4)	0.298 (1)	0.442 (1)	0.5
Si	<i>x</i>	0.4268(1)	0.4270(1)	0.4272(1)	0.4275(1)	0.4280(1)	0.4280(1)	0.4281(1)
	<i>y</i>	0.0943(1)	0.0945(1)	0.0946(1)	0.0947(1)	0.0947(1)	0.0948(1)	0.0948(1)
	<i>z</i>	0.25	0.25	0.25	0.25	0.25	0.25	0.25
	<i>B</i>	0.30 (1)	0.32 (1)	0.34 (1)	0.33 (1)	0.42 (1)	0.33 (1)	0.40 (1)
O1	<i>x</i>	0.7663(2)	0.7667(2)	0.7668(2)	0.7672(3)	0.7674(3)	0.7663(4)	0.7675(4)
	<i>y</i>	0.0923(1)	0.0925(1)	0.0927(1)	0.0930(1)	0.0930(2)	0.0926(2)	0.0922(2)
	<i>z</i>	0.25	0.25	0.25	0.25	0.25	0.25	0.25
	<i>B</i>	0.44 (1)	0.44 (1)	0.47 (1)	0.47 (2)	0.54 (2)	0.48 (2)	0.54 (3)
O2	<i>x</i>	0.2189(2)	0.2178(2)	0.2164(2)	0.2159(3)	0.2158(3)	0.2155(4)	0.2150(4)
	<i>y</i>	0.4473(1)	0.4473(1)	0.4477(1)	0.4478(1)	0.4480(1)	0.4485(2)	0.4486(2)
	<i>z</i>	0.25	0.25	0.25	0.25	0.25	0.25	0.25
	<i>B</i>	0.44 (1)	0.47 (2)	0.47 (1)	0.48 (2)	0.55 (2)	0.50 (3)	0.55 (3)
O3	<i>x</i>	0.2786(1)	0.2791(2)	0.2796(1)	0.2800(2)	0.2805(2)	0.2811(2)	0.2815(2)
	<i>y</i>	0.1635(1)	0.1636(1)	0.1640(1)	0.1639(1)	0.1641(1)	0.1641(1)	0.1642(1)
	<i>z</i>	0.0333(1)	0.0335(1)	0.0337(1)	0.0339(1)	0.0334(2)	0.0337(2)	0.0241(2)
	<i>B</i>	0.47 (1)	0.48 (1)	0.51 (1)	0.50 (1)	0.60 (2)	0.51 (2)	0.51 (2)

^aIsotropic equivalent of the anisotropic temperature factors (Ref. 18). ^b0.5 represents full occupancy.

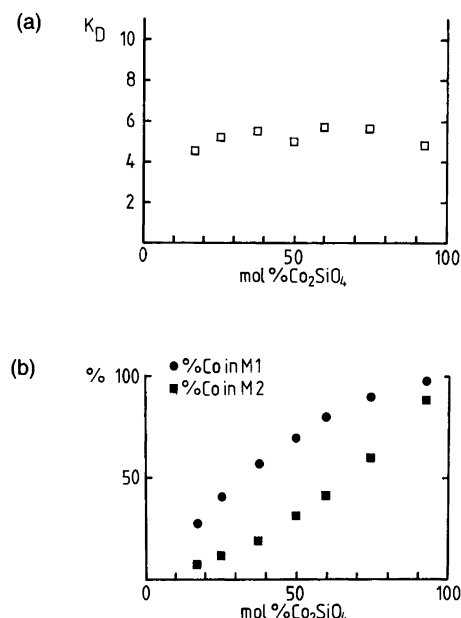


Fig. 1. Variation of (a) the intracrystalline distribution constant K_D (see text) and (b) the Co^{2+} content in M1 and M2 with composition.

effect on the ordering is relatively small in this solid solution. However, it is more plausible that the ordering found previously for the olivines synthesized at 1150 °C⁹ and at 1540 °C¹⁰ reflects the situation at lower temperatures, due to a relatively high cation diffusion rate and slow cooling of the crystals. Thus, the K_D values from the previous investigations reflect the partitioning of the divalent cation at temperatures around 1000 °C.

The occupancy results can be used to calculate the activity of $\text{CoSi}_{0.5}\text{O}_2$ in the (Co,Mg)-olivine solid solution. From statistical thermodynamics and assuming ideal mixing on each of the two octahedral sites, the following relationship can be derived⁷:

$$a(\text{CoSi}_{0.5}\text{O}_2) = (\text{Co}_{\text{M}1} \cdot \text{Co}_{\text{M}2})^{1/2}$$

where $\text{Co}_{\text{M}1}$ and $\text{Co}_{\text{M}2}$ represent the fractional occupancy of the M1 and M2 sites, respectively, by Co^{2+} (the unit $\text{CoSi}_{0.5}\text{O}_2$ is chosen here since $a(\text{CoSi}_{0.5}\text{O}_2)$ in the ideal case is linearly dependent on the composition). The calculated values are plotted in Fig. 2. The cation ordering results in negative deviations from a Raoult's law behaviour at 1173K (900 °C). A "macroscopic" activity investigation by Seifert

Table 4. Anisotropic temperature factor coefficients ($\beta_{ij} \cdot 10^4$).

		$X(\text{Co}^{2+})$							
Atom	ij	0.175	0.258	0.377	0.503	0.604	0.745	0.929	1.000
M1	11	377(12)	359(11)	423(10)	454(10)	540(18)	426(14)	417(15)	319(14)
	22	142(3)	113(2)	118(2)	124(2)	160(4)	138(3)	150(3)	122(3)
	33	257(7)	265(7)	287(6)	260(6)	326(11)	361(9)	352(9)	319(9)
	12	- 1(3)	- 2(3)	- 2(2)	1(3)	- 1(3)	- 3(4)	- 2(3)	2(3)
	13	-39(6)	-38(6)	-40(4)	-35(6)	-41(5)	-22(6)	-31(5)	-35(5)
	23	-37(3)	-35(3)	-35(2)	-35(2)	-33(3)	-37(3)	-36(3)	-36(2)
M2	11	430(17)	432(17)	542(15)	559(16)	572(23)	522(17)	514(16)	421(13)
	22	104(3)	80(3)	86(3)	93(3)	116(5)	108(3)	113(3)	80(3)
	33	328(10)	293(10)	316(9)	292(9)	304(15)	394(11)	394(10)	345(9)
	12	3(5)	6(5)	1(4)	7(5)	6(5)	8(5)	5(4)	8(3)
Si	11	199(12)	264(13)	331(12)	324(15)	413(22)	267(21)	287(23)	187(21)
	22	96(3)	78(3)	80(2)	85(3)	121(4)	82(4)	111(4)	77(4)
	33	232(7)	265(8)	261(7)	231(9)	263(13)	287(12)	328(13)	285(12)
	12	1(4)	4(4)	1(4)	- 4(5)	2(6)	- 1(7)	4(7)	- 8(6)
O1	11	251(26)	302(30)	329(26)	353(36)	414(42)	361(48)	353(49)	272(43)
	22	149(6)	132(7)	136(6)	145(8)	165(10)	137(10)	165(11)	133(10)
	33	337(17)	345(19)	384(16)	329(22)	379(26)	373(29)	428(30)	357(27)
	12	- 4(10)	2(12)	25(10)	14(15)	14(16)	27(18)	15(18)	27(16)
O2	11	425(26)	481(31)	547(28)	545(39)	656(47)	526(50)	537(51)	402(44)
	22	96(6)	83(6)	75(5)	93(8)	100(9)	77(9)	121(10)	83(9)
	33	370(18)	441(20)	420(17)	388(23)	447(28)	477(32)	446(33)	441(30)
	12	- 6(10)	- 4(12)	0(10)	- 14(15)	- 12(16)	- 23(18)	13(19)	- 21(16)
O3	11	413(18)	516(22)	561(19)	532(26)	631(31)	447(34)	536(37)	468(33)
	22	146(4)	122(4)	130(4)	132(5)	162(7)	146(7)	163(8)	139(7)
	33	300(12)	319(13)	334(11)	327(16)	368(18)	349(20)	367(20)	361(19)
	12	8(7)	3(8)	5(7)	- 9(10)	17(12)	1(13)	31(14)	14(12)
	13	-27(13)	-34(15)	-14(13)	-22(18)	-43(21)	17(23)	8(24)	-27(21)
	23	45(6)	40(6)	47(6)	46(8)	56(9)	40(11)	43(11)	44(10)

Table 5. Interatomic angles (°).

		$X(\text{Co}^{2+})$							
		0.175	0.258	0.377	0.503	0.604	0.745	0.929	1.000
Tetrahedron									
[1] O(1)-Si-O(2)		114.05(5)	113.90(6)	113.78(5)	113.83(7)	113.90(8)	113.70(9)	113.48(9)	113.52(8)
[2] O(1)-Si-O(3)		115.91(3)	115.86(3)	115.83(3)	115.79(4)	115.72(5)	115.78(6)	115.83(6)	115.77(5)
[2] O(2)-Si-O(3)		102.17(3)	102.33(4)	102.51(3)	102.55(4)	102.55(6)	102.58(6)	102.70(6)	102.68(5)
[1] O(3)-Si-O(3')		104.81(5)	104.78(5)	104.65(5)	104.62(6)	104.67(8)	104.72(9)	104.62(9)	104.75(8)
M1 octahedron									
[2] O(1)-M1-O(3)		84.91(3)	84.82(3)	84.73(3)	84.64(4)	84.67(5)	84.84(6)	84.76(6)	84.86(5)
[2] O(1)-M1-O(3')		95.09(3)	95.18(3)	95.27(3)	95.36(4)	95.33(5)	95.16(6)	95.24(6)	95.14(5)
[2] O(1)-M1-O(2)		86.83(3)	86.93(3)	87.00(3)	87.06(4)	87.04(4)	87.08(5)	86.98(5)	86.94(4)
[2] O(1)-M1-O(2')		93.17(3)	93.07(3)	93.00(3)	92.94(4)	92.96(4)	92.92(5)	93.02(5)	93.06(4)
[2] O(2)-M1-O(3')		105.30(3)	105.38(3)	105.57(3)	105.66(4)	105.65(5)	105.83(5)	105.93(5)	105.90(5)
[2] O(2)-M1-O(3)		74.70(3)	74.62(3)	74.43(3)	74.34(4)	74.35(5)	74.17(5)	74.07(5)	74.10(5)
M2 octahedron									
[2] O(1)-M2-O(3'')		90.80(3)	90.86(3)	90.84(3)	90.92(3)	90.94(4)	90.95(4)	91.13(4)	91.13(4)
[2] O(1)-M2-O(3)		81.31(3)	81.39(3)	81.53(3)	81.58(4)	81.63(5)	81.71(5)	81.57(5)	81.59(4)
[2] O(2)-M2-O(3)		96.78(3)	96.77(3)	96.87(3)	96.90(4)	96.88(5)	96.94(5)	97.02(5)	97.03(4)
[2] O(2)-M2-O(3'')		90.56(3)	90.44(3)	90.29(3)	90.15(3)	90.11(4)	90.00(4)	89.86(4)	89.83(4)
[1] O(3)-M2-O(3')		71.71(4)	71.60(4)	71.56(3)	71.44(5)	71.53(6)	71.40(6)	71.22(6)	71.33(6)
[2] O(3)-M2-O(3'')		88.66(2)	88.65(2)	88.61(2)	88.66(2)	88.61(3)	88.62(3)	88.66(3)	88.62(3)
[1] O(3'')-M2-O(3'')		110.26(4)	110.42(4)	110.57(4)	110.62(5)	110.65(6)	110.77(7)	110.88(7)	110.86(6)

^aThe number in the square brackets refers to the multiplicity of the angle.

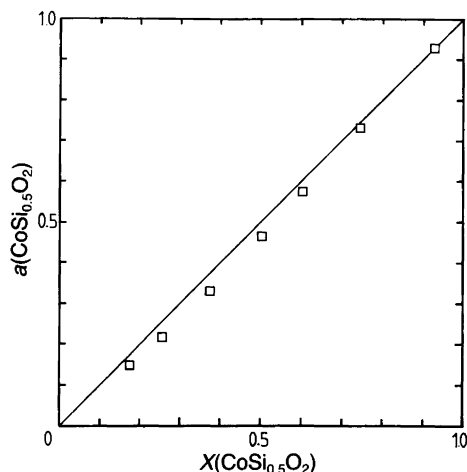


Fig. 2. Activity vs. olivine composition at 1173K.

and O'Neill¹⁴ of this solid solution series at 1573K suggested the activity–composition relation to be close to ideal or slightly positive. According to the activity relation given above, any ordering on the two octahedral sites M1 and M2 would result in negative activities. Thus, even if the ordering effect at 1573K can be expected to be smaller than at 1173K, the two-site ordering only cannot explain the “macroscopic” activities as given by Seifert and O'Neill.¹⁴

M1-octahedra. The individual and mean M1-O distances all show positive deviations from linearity with respect to the composition (Fig. 3, Table 6). This is also the case with the

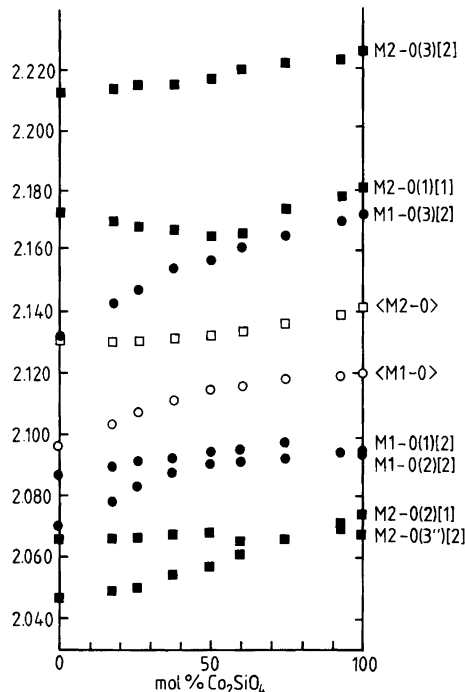


Fig. 3. Variation of octahedral metal-oxygen distances with composition. Figures in square brackets refer to the multiplicity of the bond.

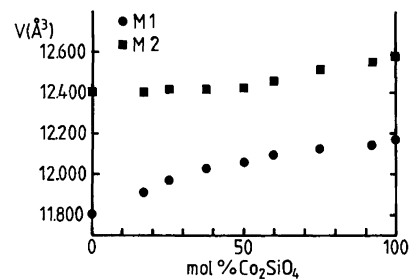


Fig. 4. Volumes of the M1 and M2 octahedra vs. composition.

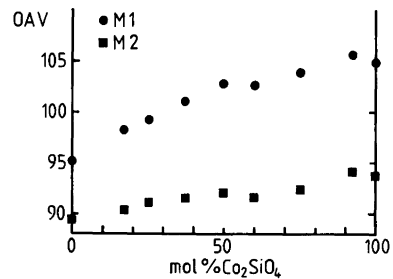


Fig. 5. Variation of the octahedral distortion parameter, OAV, with composition (see Table 7 for definitions).

octahedral volumes (Fig. 4, Table 7) and the octahedral angle distortion parameter *OAV*¹⁵ (Fig. 5, Table 7). These trends are expected, considering the preference of the larger Co²⁺ ion ($r = 0.745 \text{ \AA}$)¹⁶ for the M1-site (Fig. 1b). This reasoning, however, could not be applied to the analog-

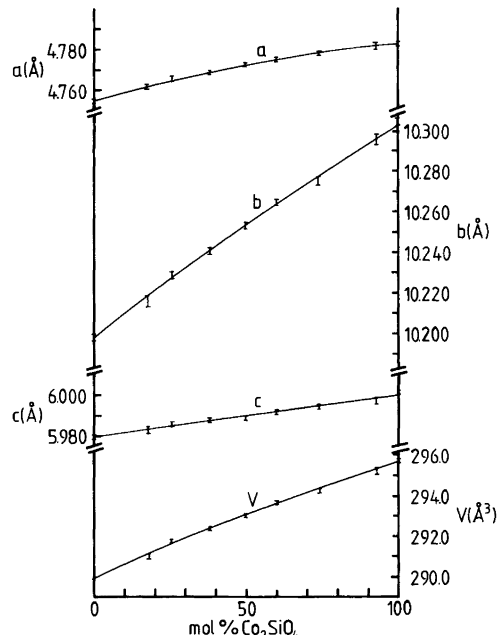


Fig. 6. Variation in the unit-cell parameters for the (Co,Mg)-olivine solid solution. The vertical bars represent two standard deviations.

Table 6. Interatomic distances (Å).

	X(Co ²⁺)							
	0.175	0.258	0.377	0.503	0.604	0.745	0.929	1.000
Tetrahedron								
[1]*Si-O(1)	1.617(1)	1.619(1)	1.619(1)	1.621(1)	1.621(2)	1.617(2)	1.623(2)	1.622(2)
[1] Si-O(2)	1.655(1)	1.657(1)	1.653(1)	1.654(1)	1.655(2)	1.653(2)	1.654(2)	1.654(2)
[2] Si-O(3)	1.636(1)	1.636(1)	1.636(1)	1.635(1)	1.639(1)	1.637(1)	1.636(1)	1.639(2)
<Si-O>	1.636	1.637	1.636	1.636	1.639	1.636	1.637	1.639
[1] O(1)-O(2)	2.745(1)	2.746(1)	2.741(1)	2.744(2)	2.746(2)	2.738(2)	2.740(3)	2.740(2)
[2] O(1)-O(3)	2.758(1)	2.759(1)	2.758(1)	2.758(1)	2.760(2)	2.756(2)	2.761(2)	2.762(2)
[2] O(2)-O(3)	2.561(1)	2.565(1)	2.565(1)	2.566(1)	1.570(2)	2.567(2)	2.569(2)	2.571(2)
[1] O(3)-O(3)	2.593(1)	2.592(1)	2.590(1)	2.588(2)	2.595(2)	2.593(2)	2.589(2)	2.596(2)
<O-O>	2.662	2.664	2.663	2.663	2.667	2.663	2.665	2.667
M1 octahedron								
[2] M1-O(1)	2.089(1)	2.091(1)	2.093(1)	2.094(1)	2.095(1)	2.097(1)	2.094(1)	2.095(1)
[2] M1-O(2)	2.078(1)	2.083(1)	2.087(1)	2.090(1)	2.091(1)	2.092(1)	2.094(1)	2.094(1)
[2] M1-O(3)	2.142(1)	2.147(1)	1.154(1)	2.157(1)	2.161(1)	2.165(1)	2.170(1)	2.172(1)
<M1-O>	2.103	2.107	2.111	2.114	2.116	2.118	2.119	2.120
[2] O(1)-O(3)	2.856(1)	2.858(1)	2.862(1)	2.863(1)	2.867(2)	2.876(2)	2.875(2)	2.880(2)
[2] O(1)-O(3')	3.122(1)	3.129(1)	3.138(1)	3.143(1)	3.147(2)	3.147(2)	3.150(2)	3.150(2)
[2] O(1)-O(2)	2.864(1)	2.871(1)	2.877(1)	2.881(2)	2.882(2)	2.886(2)	2.882(3)	2.882(2)
[2] O(1)-O(2')	3.027(1)	3.029(1)	3.032(1)	3.033(1)	3.035(1)	3.036(1)	3.038(1)	3.040(1)
[2] O(2)-O(3')	3.355(1)	3.365(1)	3.377(1)	3.384(1)	3.388(2)	3.396(2)	3.404(2)	3.405(2)
[2] O(2)-O(3)	2.561(1)	2.565(1)	2.565(1)	2.566(1)	2.570(2)	2.567(2)	2.569(2)	2.571(2)
<O-O>	2.964	2.970	2.975	2.978	2.982	2.985	2.986	2.988
M2 octahedron								
[1] M2-O(1)	2.170(1)	2.168(1)	2.167(1)	2.165(1)	2.166(2)	2.174(2)	2.178(2)	2.181(2)
[1] M2-O(2)	2.049(1)	2.050(1)	2.054(1)	2.057(1)	2.061(2)	2.066(2)	2.071(2)	2.074(2)
[2] M2-O(3)	2.214(1)	2.215(1)	2.215(1)	2.217(1)	2.220(1)	2.22201)	2.223(1)	2.226(1)
[2] M2-O(3')	2.066(1)	2.066(1)	2.067(1)	2.068(1)	2.065(1)	2.066(1)	2.069(1)	2.068(1)
<M2-O>	2.130	2.130	2.131	2.132	2.133	2.136	2.139	2.141
[2] O(1)-O(3'')	3.017(1)	3.017(1)	3.017(1)	3.018(1)	3.017(2)	3.024(2)	3.033(2)	3.035(2)
[2] O(1)-O(3)	2.856(1)	2.858(1)	2.862(1)	2.863(1)	2.867(2)	2.876(2)	2.875(2)	2.880(2)
[2] O(2)-O(3)	3.189(1)	3.191(1)	3.196(1)	3.200(1)	3.205(2)	3.212(2)	3.218(2)	3.223(2)
[2] O(2)-O(3''')	2.924(1)	2.922(1)	2.921(1)	2.921(1)	2.920(2)	2.922(2)	2.924(2)	2.924(2)
[1] O(3)-O(3')	2.593(1)	2.592(1)	2.589(1)	2.588(2)	2.595(2)	2.593(2)	2.589(2)	2.596(2)
[2] O(3)-O(3'')	2.992(1)	2.994(1)	2.992(1)	2.996(1)	2.995(1)	2.998(1)	3.001(2)	3.002(2)
[1] O(3'')-O(3''')	3.390(1)	3.394(1)	3.398(1)	3.400(2)	3.396(2)	3.401(2)	3.408(2)	3.405(2)
<O-O>	2.995	2.996	2.997	2.999	3.000	3.005	3.008	3.011

^aThe number in square brackets refers to the multiplicity of the bond.

Table 7. Polyhedral distortion parameters ^a and octahedral volumes (V_{M1} and V_{M2}).

	X(Co ²⁺)							
	0.175	0.258	0.377	0.503	0.604	0.745	0.929	1.000
V_{M1} Å ³	11.908(7)	11.965(6)	12.027(6)	12.057(7)	12.095(8)	12.126(10)	12.142(10)	12.169(8)
V_{M2} Å ³	12.407(6)	12.419(7)	12.418(6)	12.437(7)	12.458(9)	12.513(11)	12.550(11)	12.580(9)
TAV	46.4 (1)	45.0 (2)	43.9 (1)	43.6 (2)	43.3 (3)	43.0 (3)	42.4 (3)	42.1 (2)
OAV _{M1}	98.2 (1)	99.2 (1)	101.5 (1)	102.8 (2)	102.6 (2)	103.9 (2)	105.6 (2)	104.9 (2)
OAV _{M2}	90.3 (2)	91.0 (2)	91.5 (1)	92.0 (2)	91.6 (2)	92.4 (3)	94.1 (3)	93.7 (2)

^aTAV (tetrahedral-angle-variance) = $\sum_{i=1}^6 (A_i - 109.47)^2/5$, where A_i values are the tetrahedral angles O-T-O.

OAV (octahedral-angle-variance) = $\sum_{i=1}^{12} (A_i - 90)^2/11$, where A_i values are the octahedral angles O-M-O.

gous case of the (Ni,Mg)-olivines, where the *OAV* was the only parameter to follow the expected trend.

The two bonds M1-O(1) and M1-O(2), which differ by 0.016 Å in Mg₂SiO₄, are almost identical in Co₂SiO₄ (Fig. 3). This behaviour was also recognized in the (Ni,Mg)-olivine⁸ and may be due to a common coordination property of the two transition metal ions Ni²⁺ and Co²⁺ at the olivine M1 site.

M2-octahedra. The M2 volume, and the mean and individual M2-O distances all follow the expected trends. In this case, this implies positive deviations from linearity as a function of composition, $X(\text{Co}^{2+})$. The M2-O(3") bond is an exception, however, since it shows no significant change. Neither does the variation in OAV_{M2} follow the expected trend.

The distortion parameters, *OAV*, for both the M1 and M2 sites agree fairly well with those presented by Miyake *et al.*¹⁰ This also applies to the individual and mean M-O distances.

Si-tetrahedra. The mean Si-O distances are almost constant throughout the entire composition range, varying between 1.636 Å and 1.639 Å. This represents no deviation from the grand mean Si-O distance of 1.636 ± 0.004 Å, as reported by Brown.¹ The tetrahedral angle variance, *TAV*, (Table 7) decreases as a function of $X(\text{Co}^{2+})$, indicating that the SiO₄-tetrahedra become more regular as the Co²⁺ content increases. A comparison with the (Ni,Mg)-olivine system shows that *TAV* decreases in the order Ni₂SiO₄, Mg₂SiO₄, with values of 52.8, 48.1 and 42.1 respectively. At the same time the *OAV*'s increase, implying that the octahedra become more distorted for greater divalent-cation radii.

Cell parameters. All changes in cell parameters with composition are close to linear (Fig. 6). However, small positive deviations can be seen for the *a*- and *b*-axis and for the cell volume. These values show good agreement with the cell parameters presented by Matsui and Syono.¹⁷ The "drastic" increase in the length of the *b*-axis in the range from 40 to 70 mol % Co₂SiO₄, reported by Miyake *et al.*,¹⁰ is not confirmed in the present work.

Conclusion

In the (Co,Mg)-olivine solid solution, Co²⁺ shows preference for the smaller M1 site. The K_D values for the olivines investigated, which are assigned an equilibrium temperature of 900 °C, vary between 4.5 and 5.7. The compositional dependence found for the (Ni,Mg)-olivine solid solution⁸ is not found for the (Co,Mg)-olivine system. The octahedral geometric properties (such as mean and individual M-O distances, volume and distortion parameters) can in general be correlated to the cation content of each octahedron.

Acknowledgements. The author wishes to thank Professors Erik Rosén and John O. Thomas for valuable discussions and helpful suggestions. Thanks are also due to Professor Alberto Dal Negro for the microprobe analysis performed in Padova. Financial support from the Swedish Natural Science Research Council is gratefully acknowledged.

References

1. Brown, G. E., Jr. *Min. Soc. Am. Rev. Mineral.* 5 (1980) 276.
2. Lumpkin, G. R. and Ribbe, P. H. *Am. Mineral.* 68 (1983) 164.
3. Finger, L. W. *Carnegie Inst. Wash. Year Book* 69 (1970) 302.
4. Brown, G. E. and Prewitt, C. T. *Am. Mineral.* 58 (1973) 577.
5. Basso, R., Dal Negro, A., Della Guista, A. and Rossi, G. *N. Jahrb. Mineral. Monat.* (1979) 197.
6. Rajamani, V., Brown, G. E. and Prewitt, C. T. *Am. Mineral.* 60 (1975) 292.
7. Bish, D. L. *Am. Mineral.* 66 (1981) 770.
8. Boström D. *Am. Mineral.* 72 (1987) 965.
9. Ghose, S. and Wan, C. *Contrib. Mineral. Petrol.* 47 (1974) 131.
10. Miyake, M., Nakamura, H., Kojima, H. and Marumo, F. *Am. Mineral.* 72 (1987) 594.
11. Princivalle, F. and Secco, L. *Tschermaks Mineral. Petrol. Mitteil.* 34 (1985) 105.
12. Lundgren, J. O. *Crystallographic Computer Programs*, Report UUIC-B13-4-05, Institute of Chemistry, University of Uppsala, Uppsala, Sweden 1982.
13. *International Tables for X-Ray Crystallography*, Kynoch Press, Birmingham 1974, Vol IV.
14. Seifert, S. and O'Neill, H. St. C. *Geochim. Cosmochim. Acta* 51 (1987) 97.
15. Robinson, K., Gibbs, G. V. and Ribbe, P. H. *Science* 172 (1971) 567.
16. Shannon, R. D. *Acta Crystallogr., Sect. A* 32 (1976) 751.
17. Matsui, Y. and Syono, Y. *Geochem. J.* 2 (1968) 51.
18. Hamilton, W. C. *Acta Crystallogr.* 12 (1959) 609.

Received February 11, 1988.